Progress Report: Cobalt at Bornite

Zach Mahaffey, Rainer Newberry

University of Alaska, Department of Geosciences, Fairbanks Alaska USA

Cobalt is a critical and strategic element, used in a variety of technical applications. Cobalt deposits are rare outside of war-torn central Africa, however, and the international community has long searched for new sources. The Bornite Cu-Co deposit in the SW Brooks Range foothills is one such source. Getting the cobalt out of the deposit, however, is complicated by the multiple minerals and modes of occurrents. Bornite, formerly known as Ruby Creek, has been known since the 1960's to contain Co as cobaltiferous pyrite (Co-pyrite) and carrollite (ideally, $CuCo_2S_4$) and also (since 2013) as cobaltite (ideally, CoAsS). However, the distribution and mineralogical associations have been poorly constrained. The importance of better knowing such is that metallurgical testing indicates that carrollite and cobaltite report to the copper concentrate; Co-pyrite does not.

We are determining mineral compositions, relationships, and spatial distributions through: 1) detailed handheld XRF analyses of >2 km of drill core (at 5-10 cm intervals) followed by sample selection and polished section preparation and then 2) reflected light microscopy and subsequent Electron Probe Microanalyzer (EPMA) study (quantitative analyses & detailed Co maps). We have nearly completed the HHXRF studies and are about 1/3 of the way through petrography and microprobe analyses. We selected 15 drill holes that compose two cross sections: one through the historic deposit composed of the Upper and Lower Reefs (NW section) and one through the more recently discovered South Reef (SW section).

The occurrence and distribution of Co minerals and their apparent relations to other sulfides has been complicated by regional deformation events, evidenced by thrust sheets and at least 1 internal thrust (Table 1). The Bornite carbonate sequence, which hosts the sulfide mineralization, is Late Silurian to Early Devonian, as indicated by conodonts (Till et al., 2008). Selby et al. (2009) generated mid-Devonian $^{187}Re/^{187}Os$ ages for sulfide mineralization (Fig. 1), indicating that mineralization was epigenetic. The deposit likely experienced partial re-equilibration during the Jurassic-Cretaceous as evidenced by textural and compositional variations in sulfide minerals as well as the presence of cymrite intergrowths (cymrite is restricted to relatively high pressure and moderate temperature conditions, Graham et al., 1992; Fig. 2). Cobaltite compositions (Fig. 3) further indicate re-equilibration temperatures of approximately 400-500°C, from solid solution limits determined by Klemm (1965).

Delineating the distribution of the three Co minerals (Co-pyrite, carrollite, and cobaltite) from drill core assay data is convoluted by compositional variations of each of the Co minerals. So far, Co-enriched pyrite is restricted to assay intervals containing more than 0.3 wt.% Cu (Fig. 4). Similarly, cobaltite occurs in intervals of 0.5 wt.% to 5 wt.% Cu (Fig. 4) and does not typically occur in bornite rich intervals. Carrollite occurrence is restricted to intervals with >2 wt.% Cu (Fig. 4) and is commonly associated with bornite rich assemblages. Since Co broadly correlates with Cu (Fig. 5), Co was likely introduced with Cu-bearing fluids.

Cobaltite rarely occurs with carrollite (18% of occurrences) and infrequently occurs with bornite (12% of occurrences). Cobaltite is not the only As mineral, however; it never occurs with tennantite ($Cu_{10}(Zn,Fe)_2As_4S_{13}$), but can occur with tetrahedrite ($Cu_{10}(Zn,Fe)_2Sb_4S_{13}$) suggesting (Fig. 6) the reaction tennantite + Co-pyrite = tetrahedrite + cobaltite + pyrite. Compositions of cobaltite are highly variable, however is best described as (Co,Ni)(As,S)S; As-poor (disequilibrium) cobaltite is typically anhedral and rimmed by euhedral (equilibrium) normal As cobaltite (Fig. 7). The more stable cobaltite approaches the stoichiometric composition of $As_{.9\text{-}1}S_1$, and likely represents recrystallization during metamorphism (Fig. 3). Pyrite associated with cobaltite is sometimes depleted in Co, though usually not, but never depleted in As (Fig. 8) suggesting that pyrite is not usually the source of the Co and As needed for formation of cobaltite.

Carrollite displays two characteristic compositions depending on the associated Cu phase. Carrollite present with bornite has Co:Ni ratio of 3-20 and approximates $Cu(Co,Ni)_2S_4$ (Fig. 9). Carrollite in bornite-absent samples has a Co:Ni ratio of 1.3-10, and is best described as $(Cu,Ni)(Co,Ni)_2S_4$ (Fig.9). Unlike cobaltite, carrollite commonly occurs with tennantite in bornite rich assemblages and rarely occurs with cobaltite. The Ni content of pyrite increases with increasing Ni in the associated carrollite (Fig. 11). Pyrite associated with carrollite is neither Co or Ni depleted (Figs. 8, 12) and there is no textural evidence for the formation of carrollite at the expense of Co-rich pyrite (Fig. 10).

Pyrite in the Bornite deposit displays a wide range in compositions: in addition to Co, pyrite can be enriched in Ni, As, and to a lesser extent Cu. In addition to various compositions, there are multiple generations of pyrite. Co in pyrite frequently correlates with As (e.g., Fig. 13) although such As-rich pyrite appears (so far) to be rare. Conversely, Co and Cu (so far) inversely correlate (e.g., Fig. 14). Similar to the other Co bearing minerals, Co-pyrite can contain detectable Ni. However, pyrite Co:Ni ratios are extremely variable (<6 to >500), mostly due to variations in Co; most pyrite contains very little Ni (Fig. 12).

We have identified several generations of pyrite through Co mapping: the earliest is essentially Co-free and the others consistently display oscillatory Co zonation (e.g., Fig. 15). The complexity surrounding the multiple generations of pyrite highlighted by the concentric oscillatory zonation is further complicated by inclusions of other Cu minerals (Fig. 16) and less frequently (one case) microscopic cobaltite inclusions. For the SW cross section through the South Reef, there appears to be a spatial pattern of Co-pyrite sporadically throughout the Cu mineralization, with an apparent cobaltite zone higher and carrollite zone lower in the main Cu zone (Fig. 17).

Efforts continue to determine through petrography and EPMA analyses if there are consistent mineralogical zones (as suggested by Fig. 17) or if another pattern is present for Co minerals in the deposit.

Table 1: Bornite 'stratigraphy', modified from Hitzman et al. (1986) with ages from Hoiland (unpublished report).

Unit	Age	Lithology	Metamorphic Grade	Thickness
Beaver Creek	Early-Late Devonian	Phyllite, quartzite, marble	Lower Greenschist	>2000m
Upper Bornite carbonate	Early Devonian-Late Silurian	Marble, argillaceous marble, dolomitic marble, phyllite, phyllitic marble	Lower Greenschist	200-1000m
THRUST				
Phyllite - in Bornite carbonate	Late Devonian	Phyllite (PH-118)	Lower Greenschist	
Lower Bornite carbonate	Early Devonian-Late Silurian	Marble, argillaceous marble, dolomitic marble, phyllite, phyllitic marble	Lower Greenschist	200-1000m
THRUST				
Anirak schist	Permian, 287 Ma	Pelitic schist, quartzite, marble	Greenschist	3000m
THRUST				
Kogoluktuk schist	Jurassic	Pelitic schist, quartzite, marble	Epidote-Amphibolite	4000m

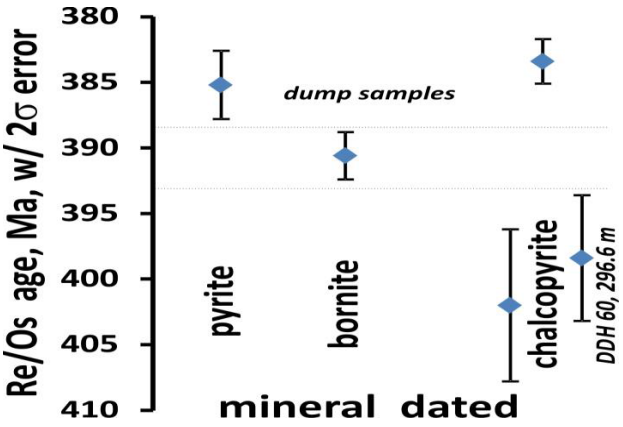

Figure 1: Highest precision 187Re/187Os ages for Ruby Creek samples, from Selby et al. (2009). These ages are inconsistent, do not coincide with apparent formation textures, and seemingly indicate a 10-15 Ma lifespan for mineralization.

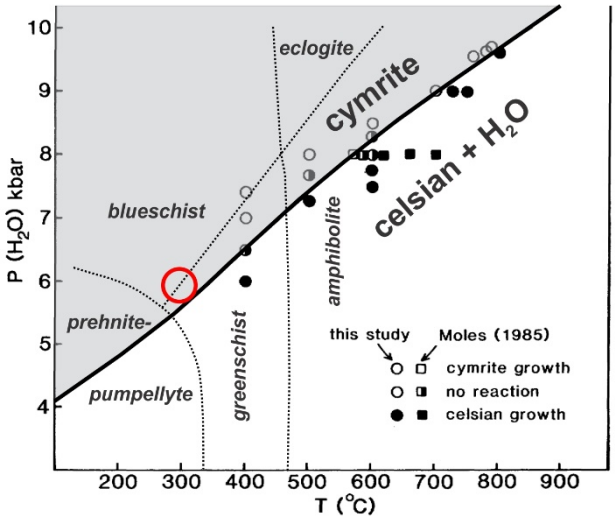

Figure 2: Stability region of cymrite (shaded) modified from Graham et al. (1992) with general boundaries between several metamorphic facies, as commonly accepted. For a minimum temperature of 300oC (from CAI) the minimum pressure conditions are approximately the red circle, near the blueschist-greenschist facies boundaries. This presumably represents the minimum metamorphic conditions experienced at Bornite.

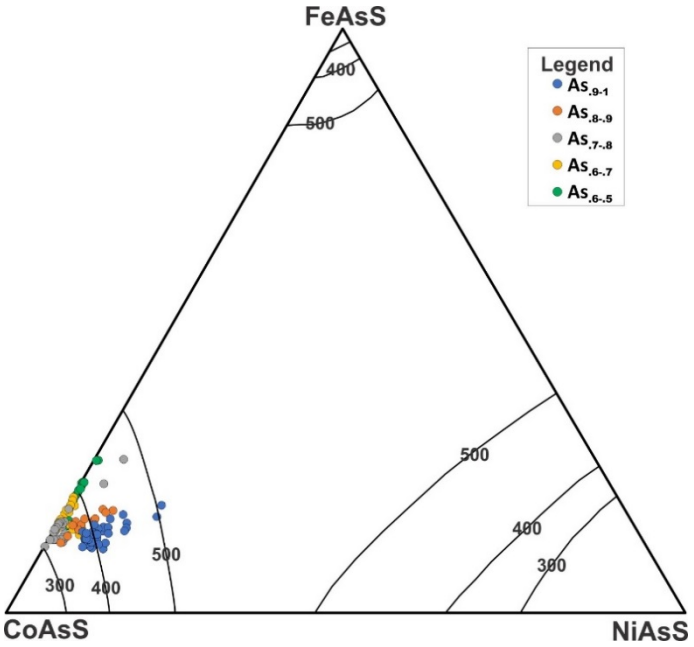

Figure 3: EPMA compositions of cobaltite from Ruby Creek plotted on the ternary diagram FeAsS-CoAsS-NiAsS. All Ruby Creek cobaltites analyzed are slightly to seriously S-enriched and As- depleted; the analyses are sorted by degree of As-deficiency. The dark blue points represent analyses closest to stoichiometric As1S1 compositions. Solid solution for those cobaltites closest to ideal As1S1 in composition indicate temperatures of 400-500℃, consistent with Upper Blueschist-Greenschist facies conditions. Modified from Klemm (1965)

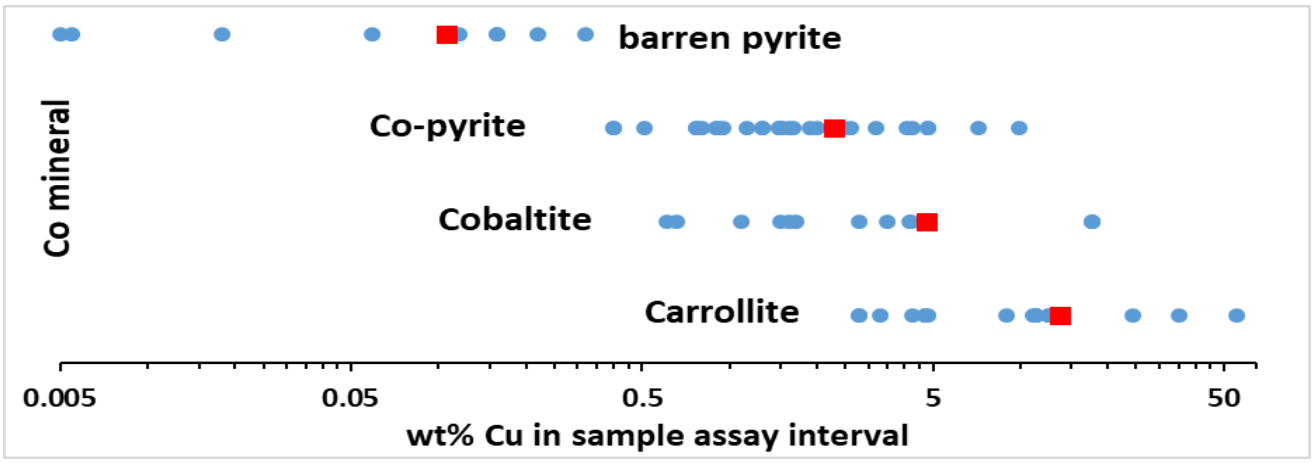

Figure 4: Blue dots represent 1 sample with EPMA verified mineralogy and the associated Cu wt.% from drill core assay. The red box represents the average Cu wt.% associated with the occurrence of each Co species.

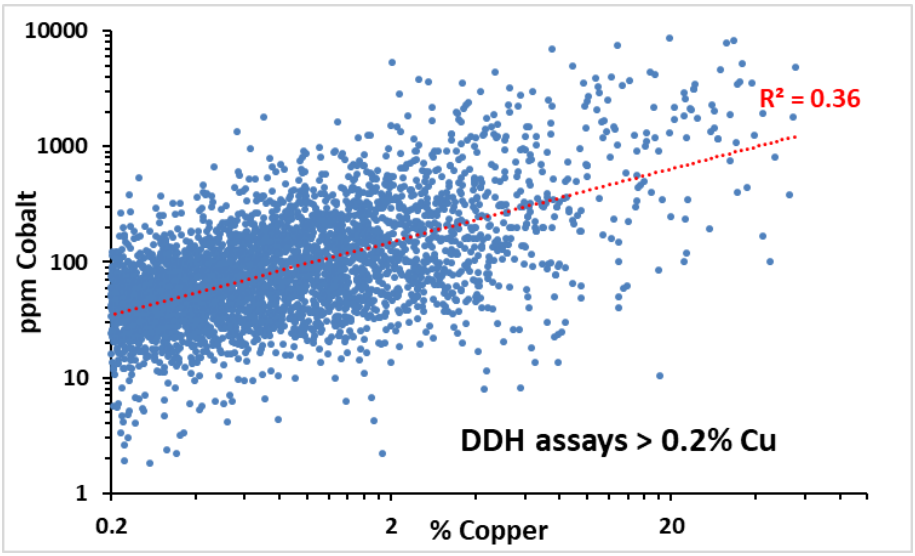

Figure 5: %Cu vs. ppm Co for drill core assays with > 0.2% Cu. The correlation between the two, present despite the occurrence of Co as Co-pyrite and cobaltite (both of which lack Cu) suggests that Cu and Co were introduced together into the Ruby Creek depo*sit*.

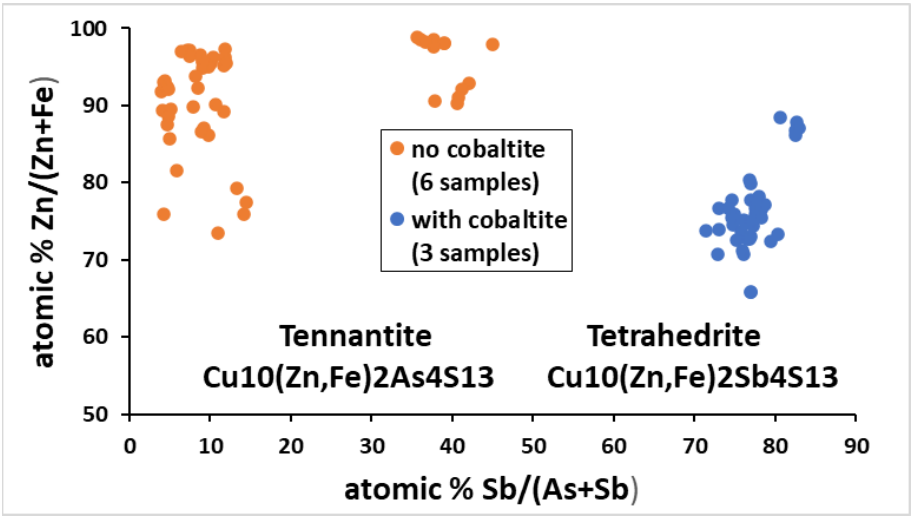

Figure 6: WDS analyses of tetrahedrite-tennantite. When cobaltite is present with fahlore the solid solution produces tetrahedrite, when cobaltite is absent tennantite is the stable phase.

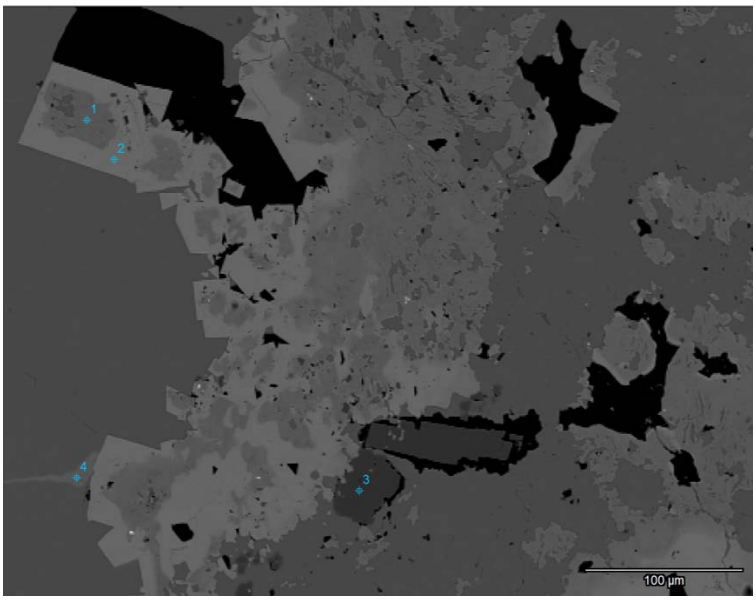

Figure 7: BSE image of euhedral, re-crystallized equilibrium (?) cobaltite (point #2), surrounding anhedral, low-As (point #1) early cobaltite. The cobaltites are surrounded by chalcopyrite (darker grey) with minor subhedral pyrite (point #3).

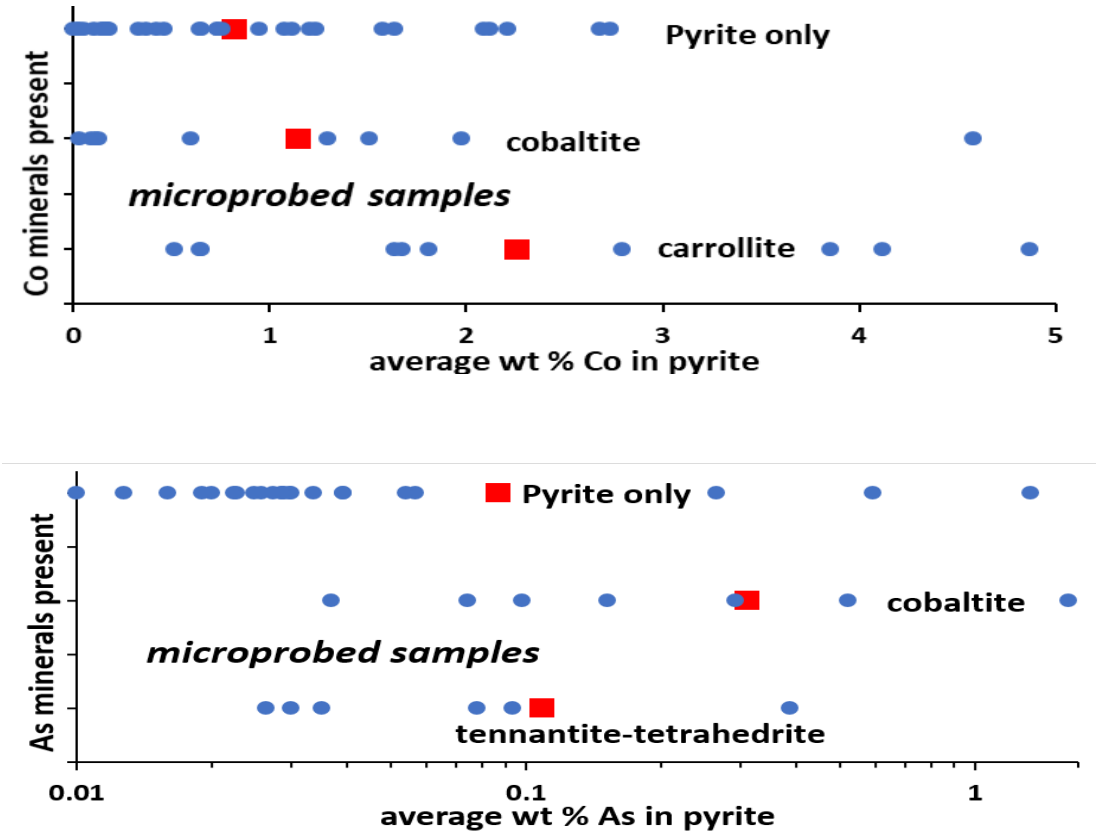

Figure 8: EMPA-determined Co (upper) and As (lower) concentrations in pyrite with different mineralogical associations.

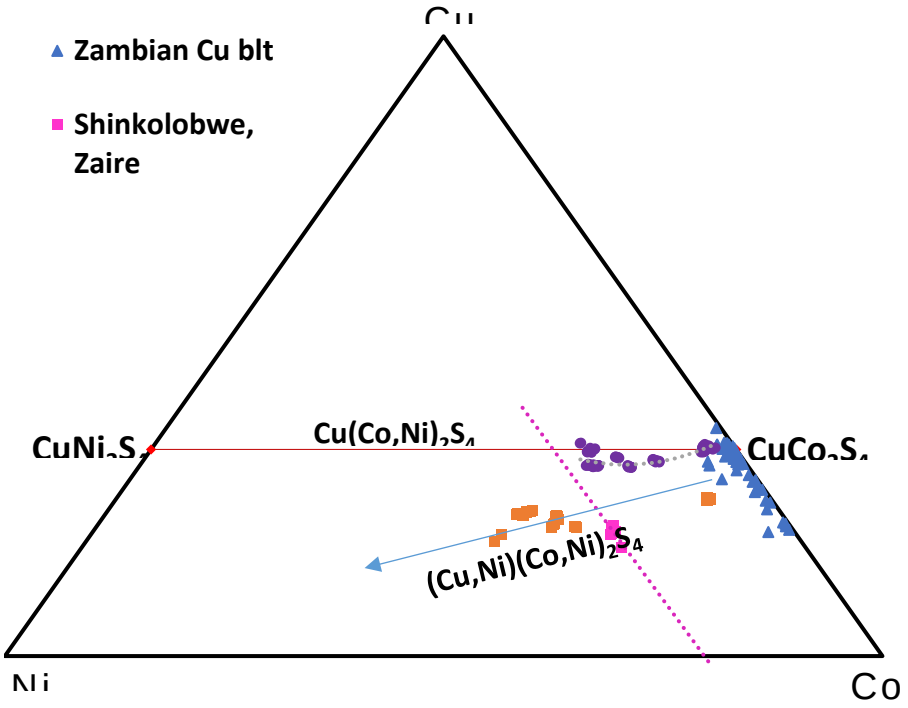

Figure 9: Carrollite compositions at Ruby Creek showing the two compositional variations. Also shown are carrollite compositions from deposits of the Congo, the leading producer of world Co.

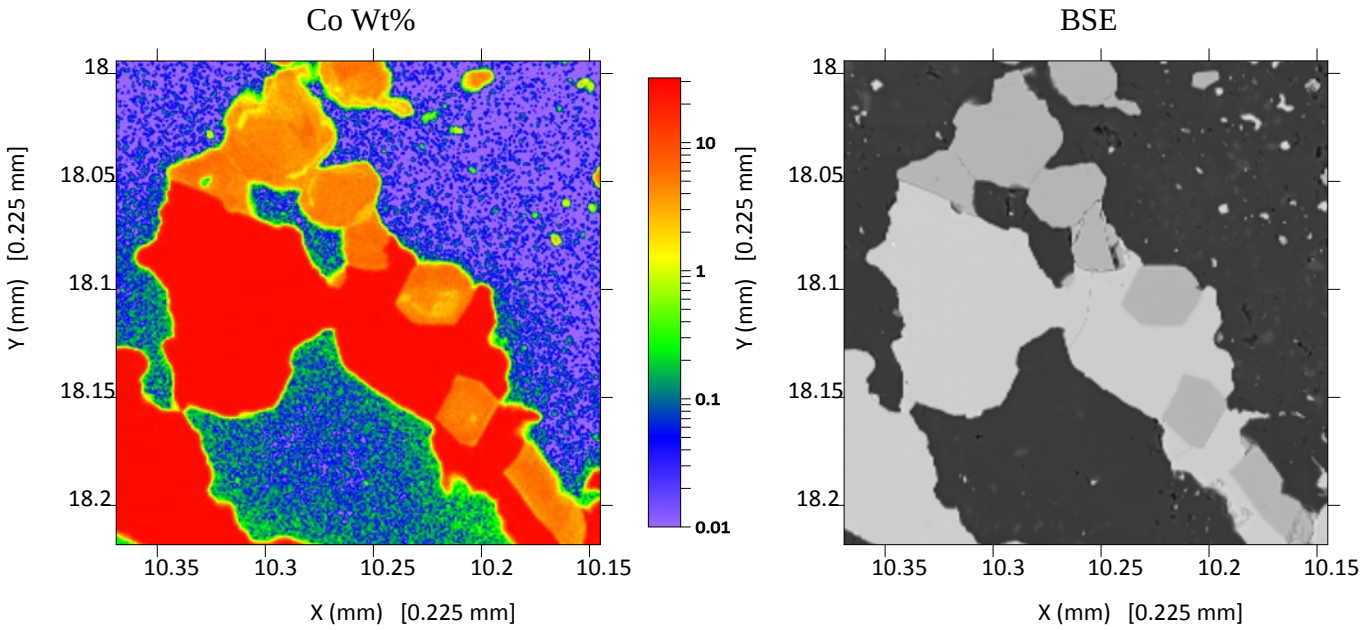

Figure 10: WDS map of carrollite (left) surrounding/adjacent to Co-rich pyrite (wt% Co as colors). The apparently elevated Co in carbonate host is likely a result of Co X-ray dispersion during analysis. BSE image (right) of the Co-mapped area for reference. Dark grey is carbonate host rock, lightest grey is carrollite and slightly darker grey is pyrite.

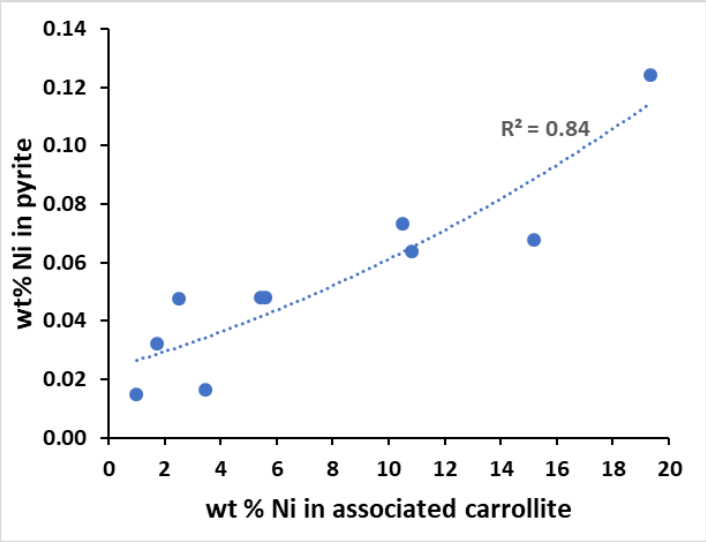

Figure 11: EMPA-based wt.% Ni in pyrite is proportional to the wt.% Ni in the associated carrollite.

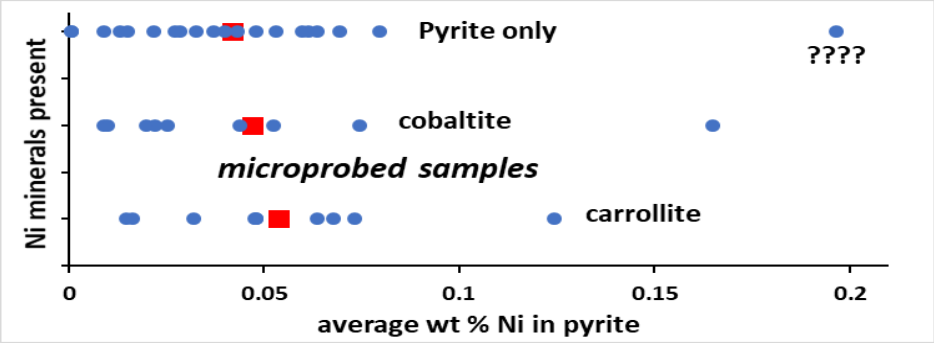

Figure 12: EMPA-based Ni contents of pyrite with different mineral assemblages. On average, pyrite associated with carrollite is slightly Ni-enriched relative to pyrite that occurs without carrollite or cobaltite.

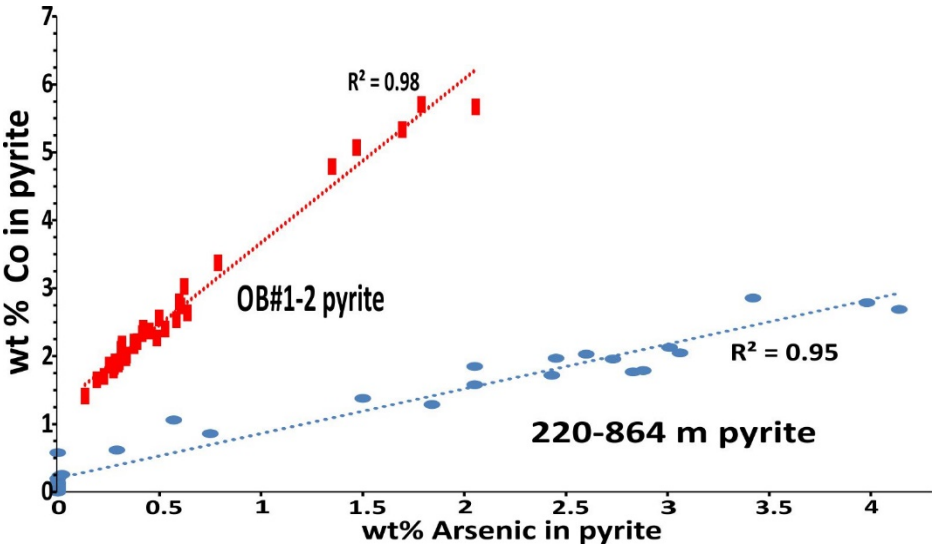

Figure 13: EMPA-based Co vs. As concentrations in pyrite for two Ruby Creek samples with high-As pyrite. So far, most Ruby Creek pyrite (Fig. 8) contains considerably less As.

Figure 14: EMPA-based inverse correlatin between Cu and Co in a relatively Cu-rich pyrite sample.

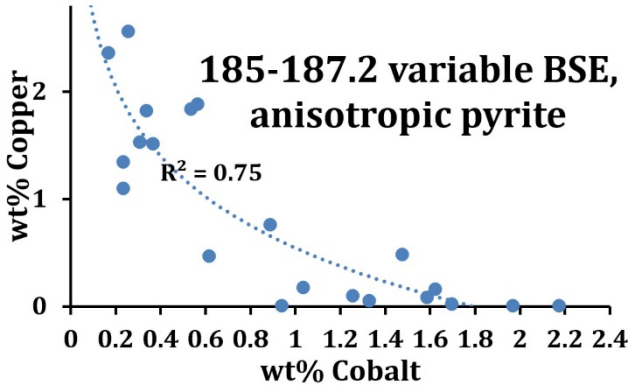

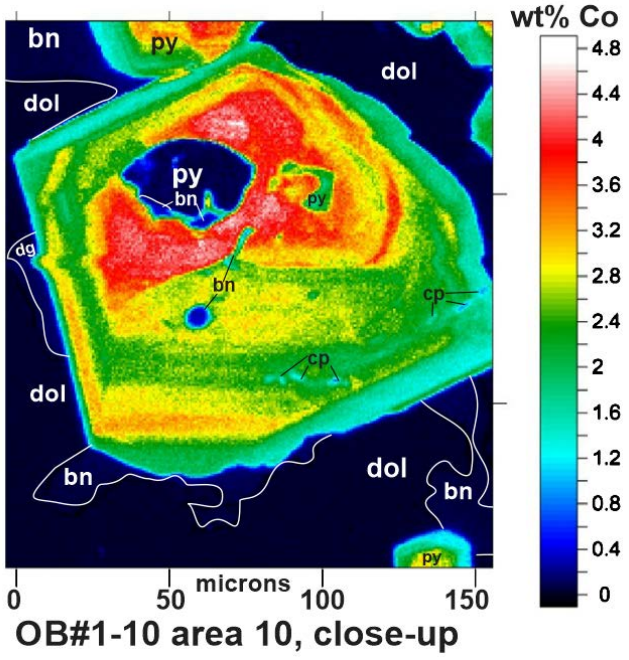

Figure 15: Co concentration map of pyrite & vicinity, showing earliest (barren) pyrite inclusion (and bornite and chalcopyrite inclusions), and later generation Co-rich pyrite. The latter commonly displays Co-enrichment towards the core and concentric oscillatory zonation. (dol = dolomite, bn = bornite, cp = chalcopyrite, py = pyrite)

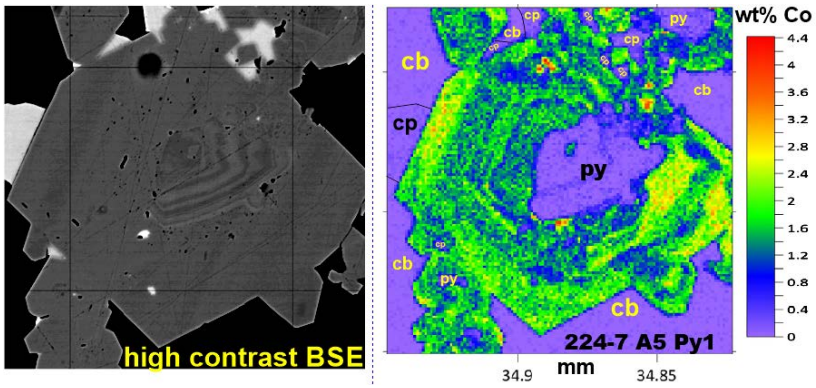

Figure 16: 2nd generation pyrite weakly Co-bearing, with distinct BSE banding (due to variable As?), surrounded by 3rd or 4th generation, oscillatory zoned pyrite. This pyrite also contains chalcopyrite (cp) inclusions (visible as bright areas in BSE image) and carbonate (cb) inclusions.

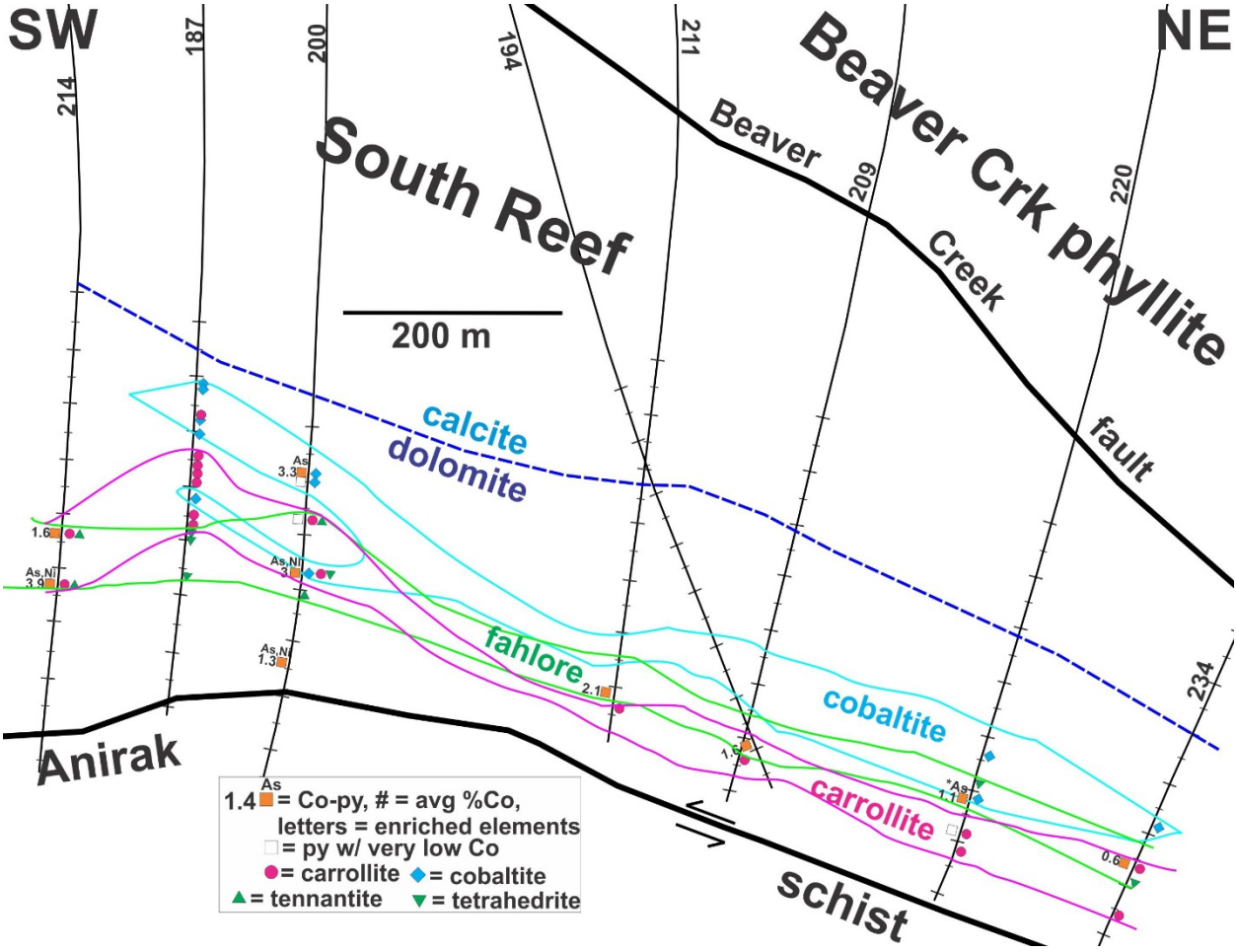

Figure 17: Generalized cross section through the South Reef showing proposed cobaltite, carrollite, and fahlore zones within Cu mineralization. Mineralogy is here is predicted from HHXRF analysis completed on drill core. Samples still need to be verified by petrographic and EPMA analyses.